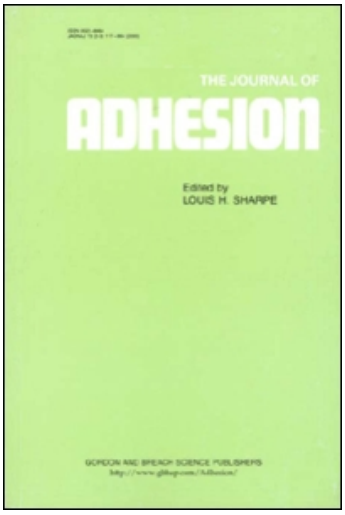

The Journal of Adhesion
Publication details, including instructions for authors and subscription information:
http://www.informaworld.com/smpp/title~content=t713453635

Measurement of the Adhesion of a Viscoelastic Sphere to a Flat Non-Compliant Substrate

Mark Reitsma[a]; Vince S. J. Craig[b]; Simon Biggs[a]
[a] The Centre for Multiphase Processes, Department of Chemistry, The University of Newcastle, Callaghan, NSW, Australia [b] The Centre for Multiphase Processes, Department of Chemical Engineering, The University of Newcastle, Callaghan, NSW, Australia

To cite this Article Reitsma, Mark , Craig, Vince S. J. and Biggs, Simon(2000) 'Measurement of the Adhesion of a Viscoelastic Sphere to a Flat Non-Compliant Substrate', The Journal of Adhesion, 74: 1, 125 — 142
To link to this Article: DOI: 10.1080/00218460008034527
URL: http://dx.doi.org/10.1080/00218460008034527

J. Adhesion, 2000, Vol. 74, pp. 125–142
Reprints available directly from the publisher
Photocopying permitted by license only

Measurement of the Adhesion of a Viscoelastic Sphere to a Flat Non-Compliant Substrate

MARK REITSMA[a], VINCE S. J. CRAIG[b] and SIMON BIGGS[a,*]

[a]*The Centre for Multiphase Processes, Department of Chemistry,* [b]*The Centre for Multiphase Processes, Department of Chemical Engineering, The University of Newcastle, Callaghan, NSW 2308, Australia*

(Received 6 April 1999; In final form 7 July 1999)

The adhesion between a single polystyrene bead (radius, 27 μm) and a flat silica surface has been measured with an atomic force microscope as a function of two variables: (a) The maximum applied load and, (b) the loading time at a constant maximum applied load. Analysis of the results indicates significant plastic deformation of the bead under the action of the load forces. There is also evidence for time-dependent viscoelastic effects as a load is exerted on the bead. The contact zone of the polystyrene bead used for these experiments was examined using Scanning Electron Microscopy. The microscope images revealed a surface covered in small polymer beads with a radius of only 115 nm. In the contact zone these beads had undergone substantial and permanent deformation as a function of the applied load. Basic geometric analysis reveals that the large sphere is not contacting the flat surface under any load. The results presented here indicate the value of being able to measure adhesion using an atomic force microscope. The importance of being able to characterise the contact zone accurately is also highlighted.

Keywords: Adhesion; Polystyrene; Silica; Viscoelastic; Plastic deformation

INTRODUCTION

The adhesion of spheres to flat surfaces is of direct relevance to a range of processes both from the industrial viewpoint and in the natural world. For example, in the natural world adhesion plays a critical role

*Corresponding author. Tel: +61 2 4921 5481, Fax: +61 2 4921 5472, e-mail: chsrb@cc.newcastle.edu.au

in processes such as blood clotting, platelet binding, and leukocyte adhesion to cell walls [1]. In the technological world, the control of adhesion has important consequences in a wide variety of processes such as drug delivery, xerography, paints, and solids handling [2]. As a result, much effort has been devoted to gaining both a theoretical understanding and experimental insights into adhesion mechanisms.

The adhesion of any sphere to a surface will depend on the area of contact at separation [3]. However, theoretical determination of this area of contact is not easy. The application of contact mechanics to problems of this type has a long history. Early work utilised simple Hertzian deformation characteristics and assumed that the spheres were elastic indentors [4, 5]. In this approach, the adhesion between the surfaces is unsustainable and the compressive stresses in the contact region lead to the conclusion that, at detachment, no tensile load is required and the area of contact is zero. These theories were subsequently enhanced to include contributions from surface forces [6]. It can be shown that these surface forces may be sufficiently large as to exceed the elastic limit of the materials and allow plastic deformations. The major problem is to decide over what areas of the interacting surfaces these forces are large enough to have a real effect. For a material that is essentially elastic under a standard load regime, two main theories have been developed. These are the so-called JKR (Johnson-Kendall-Roberts) [7] and DMT (Derjaguin-Muller-Toporov) [8] theories. The JKR approach assumes that surface forces act in the contact region but are absent outside of it. This leads to the interesting result that the tensile stresses are infinite at the edge of the contact zone. The DMT theory does allow for the action of cohesive surface forces outside of the contact zone but it assumes that these forces do not alter the shape of the material in this zone from the Hertzian profile. This results in the adhesive stress being zero in the contact region and finite in this cohesive zone. The differences between these theories are significant and lead to very different predictions. In the DMT case, the contact area – load profile is essentially equivalent to the Hertzian case offset such that at any given load the contact area will be larger. The additional surface forces result in the retention of a finite area of contact under tensile loads up to the point where detachment occurs; at this point, the contact area goes continuously to zero. The JKR case is more complex under tensile loads. As a tensile

load is applied, the contact area decreases towards a minimum, but finite, value. The retention of some contact area, even at the pull-off point under tension, is characteristic of the JKR approach.

It has been shown by Tabor [9] that these two theories apply to opposite ends of the same spectrum. The important parameter to consider is the ratio of the elastic deformation at pull-off (separation) to the range of the surface forces. For large compliant spheres, where the deformation may be substantial, this ratio is much larger than one. This is the region of application for the JKR theory. Alternatively, the DMT theory is applicable to small, stiff spheres where this ratio is less than one. Subsequently, the transition region between these two limits was investigated and complete solutions were developed [10]. A full description of the transition region between these two theories is the subject of much continuing research. In a recent paper, Johnson and Greenwood [11] presented a comprehensive adhesion map to describe the limits for each theory based on the deformation ratio and the normalised load (applied load/radius). It should be remembered, of course, that these theories and their developments are used to describe the contact of elastic bodies.

In reality, very few materials can be described as simple elastic spheres; this is especially true when we consider polymeric materials. The mechanics of contact may then be described as elastic, non-linear elastic (elasto-plastic), or plastic. In addition, time-dependent or viscoelastic effects may be important for any material under load. The type of contact mechanics that is applicable, and the extent of viscoelasticity, will be affected by the magnitude of any applied load and the time scale over which it is applied. As is clear from the above discussion, elastic contact mechanics have been extensively investigated. The plastic regime has also been the subject of investigation. Maugis and Pollock (MP) [12] developed the JKR theory to take into account plastic deformations of the interacting surfaces. The non-linear elastic or elasto-plastic regime is currently less-well described. Viscoelastic effects have also been the subject of recent research [13]. In these cases, the theories attempt to describe the change in the contact radius with time as a result of viscoelastic creep under load.

The development of new experimental techniques over the last decade has allowed a comprehensive investigation of the applicability of these theories. Clearly, the area of contact as a function of applied

load is of critical importance. The contact between atomically-smooth mica surfaces has been probed using the Surface Forces Apparatus (SFA) [14]. The results of these investigations indicated a contact area – load relationship that was well modelled by the JKR relationship. These measurements were performed between two crossed hemicylinders of mica with radii in the order of 1 cm; the material properties of mica coupled with these large radii are clearly sufficient to access the JKR regime.

Other experimental approaches have involved the use of nanoindenters [15] and scanning electron microscopy (SEM) [16, 17]. The use of SEM micrographs is an interesting approach; direct images of the contact areas and contact line deformations can be obtained as a function of time. Such images have been reported both for compliant spheres on rigid substrates and for rigid spheres on compliant substrates. The results indicate that dependent upon the nature of the system and the size of the interacting species a full range of the possible contact mechanics responses can be probed. In addition, many viscoelastic creep effects are apparent in the data.

More recently, scanning probe microscopy (SPM) techniques have been extensively used to probe surface material properties on the nanometre length scale. The majority of this research has utilised the integral tips of the simple cantilever probes to investigate these surface properties [18]. Whilst the value of this research is undoubted, certain limitations of using these probes are apparent. In general, the radius of the tip is poorly controlled and, at contact, atomic scale defects can become very important. Since application of any theory relies upon the input of a radius, this uncertainty is critical. Also, the chemistry of the tips is limited. In most cases, commercial tips are constructed from one of silicon, silicon nitride, or tungsten. Some control over these issues can be gained by attaching individual spheres of known dimensions, in the micron-size range, to the end of the cantilever springs. This opens up a virtually unlimited set of possible interaction chemistries. As well, it introduces the possibility of probing geometric effects; for example, different size ratios of interacting spheres could be used. Systems that have been studied include tin [19], xerographic toner particles [20], polystyrene [21], cross-linked polydimethylsiloxane [22], glass [23], and metal oxides [24]. In most cases, the authors reported that the measured adhesion forces at pull-off were 2 to 3 orders of magnitude

smaller than predicted from theory. This is attributed to a contact region that is dominated by surface asperities [19]. In all these early cases, the experiments were performed using springs that had a relatively weak spring constant. The load regime was such that, even for small-radius surface asperities, the yield points of the materials were not exceeded.

In a recent investigation, the effects of repeated loading and unloading cycles, (using large maximum loads) for a polystyrene microsphere on a mica surface were reported [21]. In this case, the adhesive forces recorded at pull-off were shown to be less than a factor of 3 different from the expected values using JKR theory. This improved correlation was attributed to the plastic deformation of surface asperities resulting in a contact area that was much closer to that for perfectly smooth surfaces. The loads applied were sufficient to mean that the small surface asperities were in the elasto-plastic or plastic regimes. Across the entire sphere radius the applied loads were still in the purely elastic regime.

In this paper, we extend this earlier work using a greater loading range. Again, the data presented are for a single polystyrene bead interacting with a non-compliant smooth surface. We will present direct evidence, from SEM images of the damage inflicted upon surface asperities as a result of plastic or elasto-plastic deformations. By using a variety of loading rates at a single maximum load we are also able to probe directly viscoelastic effects for the bead used here.

EXPERIMENTAL SECTION

Particle Preparation and Characterisation

The polystyrene spheres used here were prepared in-house using a standard suspension polymerisation process [25]. The resultant stable suspension of particles was cleaned by filtration through glass wool followed by dialysis against Millipore (R) water. The dialysis water was changed daily over a three-week period.

The particle size distribution was analysed using a Malvern Mastersizer S. The resultant size distribution is shown in Figure 1. It should be noted that the results show a bimodal distribution of

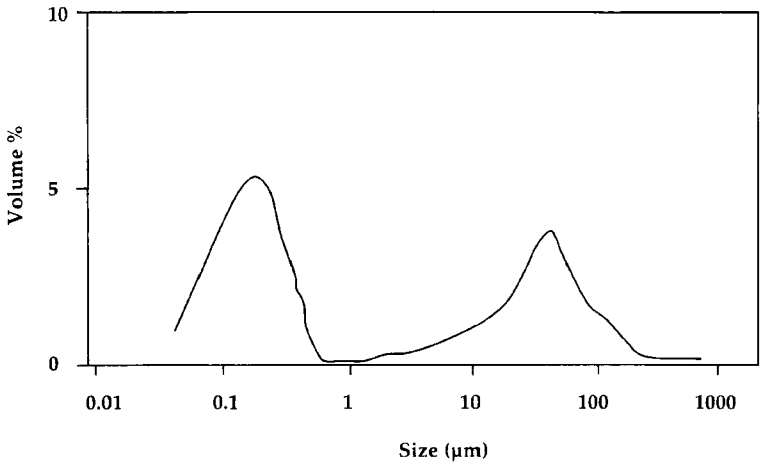

FIGURE 1 Particle size distribution plot for the polystyrene latex sample used in the adhesion measurements reported here.

particle sizes. This is not totally unexpected. The growth mechanism of particles, synthesised using suspension polymerisation, relies upon a progression from initial small polymer particles to large beads *via* an agglomeration and annealing process. The particle peak observed at a diameter of about 250 nm is, therefore, due to the presence of some unaggregated small spheres.

Probe Preparation

For ease of manipulation, and to minimise problems of glue contamination, beads with radii of between 10 and 20 μm are preferred. To facilitate preparation of the probe, a tungsten wire was etched to a fine point [26]. Using an optical microscope a single bead was selected from a drop of a diluted sample of the cleaned suspension. The wire was then used to remove the bead from this drop. Once removed, the bead quickly dried under the heat of the microscope lamp.

The isolated polymer bead was then glued to a single beam silicon cantilever (Digital Instruments, Inc.) using a small amount of epoxy resin. A scanning electron microscopy image of the colloid probe used in the studies reported here is shown in Figure 2.

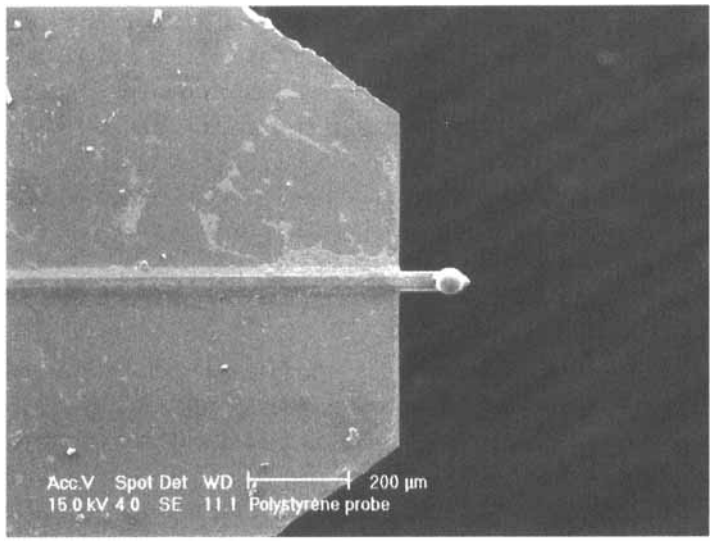

FIGURE 2 A scanning Electron Microscopy image of the colloid probe used in the measurements reported here. The probe consists of a 27.2 µm radius polystyrene bead attached to a single beam cantilever spring with a spring constant of 27 ± 1 N/m.

The spring constant of the cantilever used was determined using the technique of Cleveland *et al.* [27]. It was found to have a spring constant of 27 ± 1 N/m.

Silica Surface Preparation

The silica surfaces used in this investigation were prepared by oxidising a silicon wafer. The wafer was oxidised under an oxygen atmosphere at elevated temperatures using standard procedures. The resultant wafer had a surface oxide layer with a thickness of 140 ± 1 nm. The roughness of the surface, as determined using AFM images, was ± 2 nm over an area of 5 µm^2. The surface was cleaned by rinsing sequentially in ethanol, water and acetone followed by rapid drying under a stream of clean dry nitrogen.

SPM Force Measurements

Force-distance information was obtained from a Nanoscope ^{R} III AFM (Digital Instruments) which was operated in the "force mode".

In this mode the *X-Y* raster motion of the sample on the scanning piezoelectric crystal is suspended and the sample is moved towards and away from the cantilever in the *Z*-direction by the application of a saw-tooth voltage. In a typical experiment, the colloid probe was mounted in the commercial liquid cell (Digital Instruments). The surface used was a clean oxidised silicon wafer. AFM images indicated a surface roughness of less than $\pm$ 1 nm over an area of 1 μm^2. Prior to an experiment, the liquid cell was purged with a stream of clean dry nitrogen. During measurement, the cell was maintained under a dry nitrogen atmosphere.

Any experiment involves the silica surface being driven towards the polystyrene probe and deflections in the spring holding this probe being measured. Control of the scan size, scan rate and contact point between the surfaces allows control over the total contact time and the maximum applied load. The adhesive force is determined directly from these force-distance data as the surfaces are separated from one another.

RESULTS AND DISCUSSION

In Figure 3, data for the measured pull-off force as a function of the maximum applied load are given for the interaction between a 27.2 μm polystyrene (PS) sphere and a flat silica substrate. Two data sets are given in Figure 3, representing two consecutive loading cycles. The data in the first series show the effect of subjecting the bead to progressively increasing loads in the range from 3.5 μN to 95 μN. In this case, each run was performed after only a minimal time gap from the previous run (< 30 s). The effect of the increasing load is to cause an increase in the pull-off force for the bead from the surface. Immediately after application of the maximum load in Series 1, the applied load was reduced to $< 5\,\mu$N and a second load sweep was performed. It is clear that reducing the load did not result in the complete loss of the increased adhesion generated during the loading cycle of Series 1. Again, increasing the load during Series 2 led to an increase in the adhesive pull-off force measured.

As a comparison, data are presented in Figure 4 for the measured adhesive pull-off force between a single 41 μm radius silica sphere

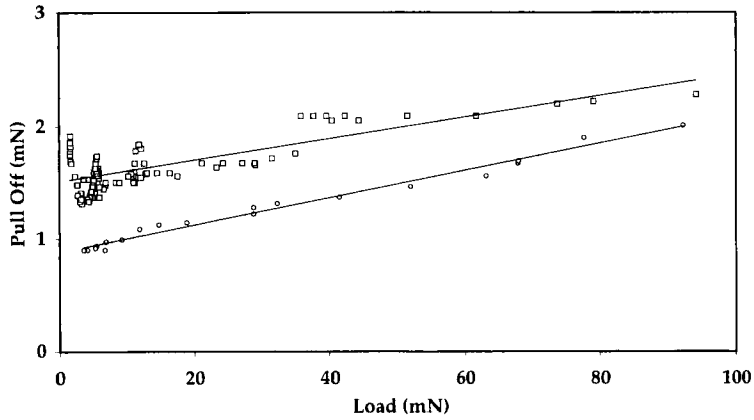

FIGURE 3 Data for the measured pull-off force *versus* applied external loading force between a 27.2 μm radius polystyrene sphere and a flat silica substrate. Two data sets are for two consecutive runs using increasing loads with the same bead and surface. The second run was started immediately the first had been completed. ○ First series, □ Second series.

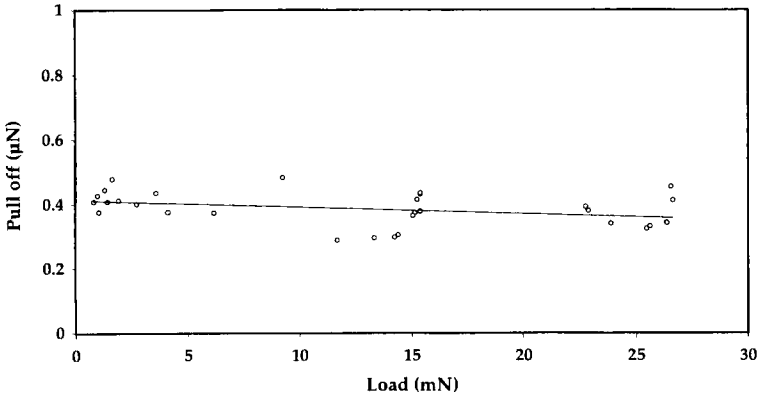

FIGURE 4 Data for the measured pull-off force *versus* applied external loading force between a 41 μm radius silica glass sphere and a flat silica substrate.

against the same silica flat. Two points are immediately apparent: the magnitude of the pull-off force is an order of magnitude smaller than in the PS case, and there is no increase in the pull-off force with increasing load.

Two important points are apparent from the load-pull-off data for the PS system. First, there must be some form of plastic or

elasto-plastic deformation of the sphere since the pull-off increases as the applied load increases. Secondly, careful analysis of the data in Series 2 indicates the partial recovery of the sphere under the lowest loads. However, it is not clear from these data if this recovery, which is due to the removal of the load, is time-independent. However, the recovery is definitely indicative of elasto-plastic effects and it may also indicate visco-elasticity. This point will be discussed in more detail later.

For the silica – silica system the results are similar to those reported previously for non-compliant elastic solids [24]. The fact that the adhesive pull-off force is invariant with applied load indicates simple elastic contact between the surfaces. For a large elastic sphere in contact with a flat solid surface, the JKR theory [7] predicts that separation will occur when

$$F_{\text{pull-off}} = -\frac{3}{2}\pi R W_{12} \tag{1}$$

R is the probe radius and W_{12} is the adhesion work term. W_{12} is often approximated using $W_{12} = 2\sqrt{\gamma_1\gamma_2}$. The calculated value of the pull-off force from this equation, using a value of $78\,\text{mJ/m}^2$ for the silica surface energy [28], is $30\,\mu\text{N}$. This value for the surface energy is at the low end of the quoted scale for silica; values as high as $350\,\text{mJ/m}^2$ have been reported [29]. Therefore, the calculated value given here should be considered as a minimum. Notwithstanding this point, the value is two orders of magnitude greater than the recorded value from the colloid probe measurements. The most probable explanation for this result is that the contact zone is dominated by surface asperities. The role of surface asperities in reducing the magnitude of the adhesion is a well-documented phenomenon [19].

The PS-silica system can be analysed in a similar way. In this case, the predicted value of the pull-off force from JKR theory, using a value of $30\,\text{mJ/m}^2$ for the PS surface energy, is $12.4\,\mu\text{N}$. This is compared with values for the pull-off of between 1 and $2\,\mu\text{N}$ measured using the colloid probe. Clearly, the measured values are much closer to the predicted values from this simple elastic theory. However, despite this close agreement, the data presented in Figure 3 indicate that this system has significant deviations from linear elastic behaviour.

The possibility of plastic deformation for the PS bead can be examined using the Maugis-Pollock (MP) [12] approach. In this theory, the conditions for the onset of elasto-plastic and full plastic behaviour are given in terms of the radius of the circle of contact: a_e and a_p, respectively.

$$a_e = \frac{4.90RY}{K} \tag{2}$$

$$a_p = \frac{60RY}{E} \tag{3}$$

in this simple theory, a dimensionless value, w^*, is defined as

$$w^* = \frac{W_{12}K^2}{RY^3} \tag{4}$$

where Y is the material yield strength and K is an elastic modulus term. Under zero applied load, when the value of w^* exceeds 5.2 the system can be assumed to be in the elasto-plastic regime. It will enter the plastic deformation zone when $w^* \geq 12000$.

The mechanical properties of polystyrene are well known [30]. Using values of $E = 2.55\,\text{GPa}$, $K = 4.3\,\text{GPa}$ and $W_{12} = 0.03\,\text{N/m}$ in the above equations, we can calculate that, for a bead of 27.2 μm radius, $w^* = 16$. Therefore, even at zero load we may expect this system to be in an elasto-plastic deformation regime.

This may possibly explain the rise in adhesion as a function of applied load. However, it should still be noted that the value of the adhesive pull-off forces at any applied load were a factor of between 5 and 10 times too small when using the simple JKR elastic theory. If we actually did have some elasto-plastic deformation in the bead, we would expect the contact area to be higher than predicted by the JKR approach and so the adhesive pull-off force should be greater than the value from the theory.

A possible explanation of why this result is obtained is to be found again in surface asperity contacts. An SEM micrograph of the bead used in this study is shown in Figure 5. Examination of this photo indicates the presence of significant surface debris. A larger scale image of the same bead is shown in Figure 6. Attention is drawn

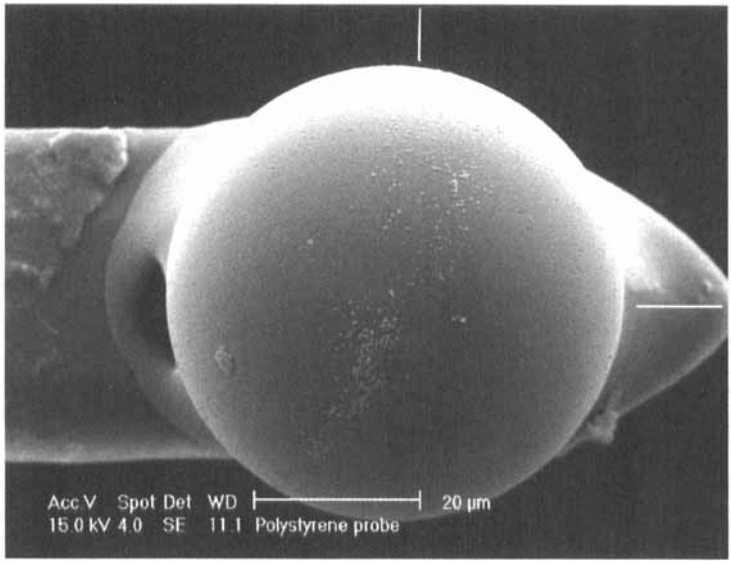

FIGURE 5 A Scanning Electron Microscopy image of the polystyrene bead used in the measurements reported here. Examination of the surface reveals the presence of significant adsorbed surface debris.

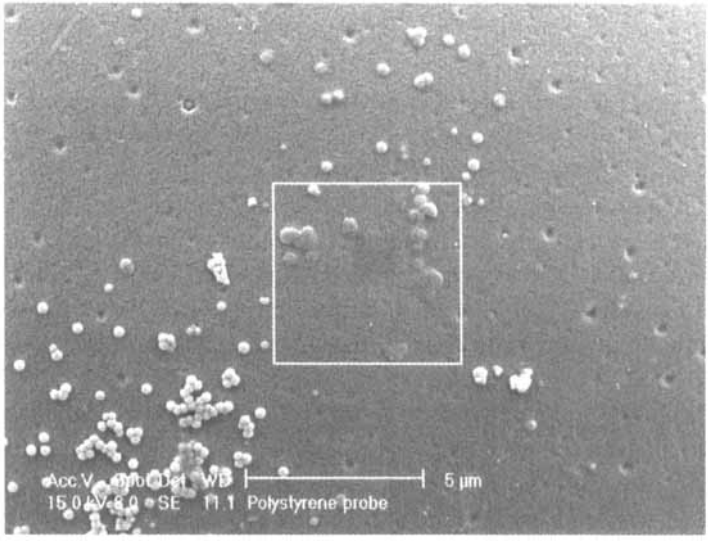

FIGURE 6 A Scanning Electron Microscopy image of the polystyrene bead showing the approximate region of contact, indicated by a white rectangle, on the surface of the polystyrene sphere at the conclusion of the loading cycles shown in Figure 3.

initially to the lower left hand corner of this image. Here, substantial numbers of small spherical particles can be seen. The sizes of these particles are approximately 230 nm. This is the size of the small residual contaminant particles that were present in our synthesised particle sample (*cf.* Fig. 1). It seems likely, therefore, that these particles are small polystyrene beads. Further evidence that these small spheres are polystyrene beads is gained from the presence of pits in the surface of the larger bead. These pits are approximately the same dimensions as the small particles and are probably positions from which, after the synthesis, partially-embedded small spheres have become dislodged. Remember that the big particles grow by agglomeration and fusion of the small spheres. In the top right corner of Figure 6 a small sphere that has become engulfed in the larger one can also be seen.

If we assume that these small spheres are indeed polystyrene beads, an interesting analysis of the contact zone can be performed. Examination of the central region of Figure 6 shows some small beads that appear to have been squashed. This region, highlighted by a white box, corresponds to the contact zone for the large sphere on the silica surface. Let us return once again to the simple JKR analysis of the expected pull-off force. However, in this case the calculation can be done assuming that the contact between the surfaces is through a single small sphere, radius = 115 nm. This results in a value for the adhesive pull-off force of 0.052 μN; our smallest measured value was approximately 1 μN. Thus, we would need around 20 of the small spheres to be contacting the silica surface at pull-off; in the SEM image there are around half this number. Two possibilities for the measured value can be postulated. In the first, there is some contribution to the overall adhesive force from the larger sphere. The second possibility is that the small spheres have undergone some plastic deformation resulting in a larger contact area and, hence, higher adhesion energy. A cursory inspection of the squashed beads in the contact zone suggests that this is the most likely explanation.

If we take the contact region, from Figure 6, to be a box with sides of 5 μm, a simple geometric analysis can be done. From Figure 7, we can see that such an analysis would result in a maximum height difference of 116 nm from the edge to the centre of this box when considering the surface of the larger sphere. The small spheres are

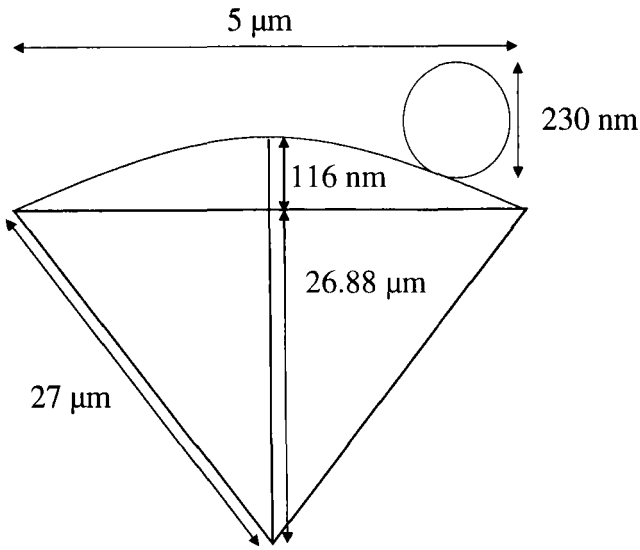

FIGURE 7 A schematic representation of the contact geometry of the sphere used in the measurements reported here. The height variation, from the edge to the centre of the curvature, across the width of the approximate contact zone (given in Fig. 6) is shown.

about twice this size. Therefore, even if the asperities were close to the edge of the box we would expect them to contact the flat surface well in advance of the large sphere surface. Indeed, a small sphere at the edge would have to deform by > 115 nm before the large sphere could have any contact. It is likely, therefore, that all of the observed adhesion is caused by these surface asperities.

A simple MP analysis using the small sphere radius predicts a value of $w^* = 3800$. Again, this is in the elasto-plastic regime. Thus, as we apply greater and greater loads, the permanent deformation will be expected to be continuously increasing and so the adhesion is seen to increase.

As we mentioned above, the data presented in Figure 3 appear to show some viscoelastic effects. After completion of the first loading run (Series 1) the system was allowed to rest for the standard 30 s. The first data point of Series 2 was collected at an applied load of 1 μN. Interestingly, this run resulted in an adhesion value that was approximately the same as the last point collected in Series 1 at 95 μN. Increasing the applied load was then seen to result initially in a

reduction in the measured adhesion up to a load of about 5 μN. After this point, in general, the adhesion data were again seen to rise as a function of applied load, as for Series 1. It should be noted, however, that the data exhibit significant scatter up to a load of about 20 μN. All of these points indicate the presence of time-dependent effects in the measured data.

The initial reduction in adhesion observed in Series 2 is directly attributable to a partial recovery of the deformed contact zone of the bead. Clearly, all of the deformation experienced by the bead at the highest load in Series 1 is unsustainable at the low loads (< 5 μN) used initially in Series 2. However, the recovery is not instantaneous and, so, we see this apparent drop in the adhesion initially in Series 2. At loads of greater than 5 μN the adhesion begins to increase again with further increases in load. Since these values are larger than the corresponding adhesion values in Series 1, the relaxation process does not permit the full recovery of the bead structure. That is, plastic deformation has occurred. At all loads in Series 2 the measured pull-of adhesion values were higher than in Series 1. This indicates that at all applied loads in Series 1 the maximum adhesion value at that load had not been achieved. In other words, the creeping flow of the bead under that applied load was not complete in the timescale of the experiment. Recent advances in experimental methodology have driven an increased activity in the theoretical description of the contact mechanics for a viscoelastic material. This is a non-trivial problem. Unertl [31] has found that the maximum area of contact for a viscoelastic material under load can occur significantly after that load was applied. This appears to be the case here.

Further information about time-dependent viscoelastic effects in the system used here was found by measuring the adhesive pull-off force as a function of loading time for a single applied load. Results for this experiment are shown in Figure 8. These data indicate clearly that the adhesion increases with loading time. It should be remembered, of course, that the results given here are for a consecutive series of loading cycles on the same bead going from short to long times. Thus, the final load must contain some compounded information from the previous runs. Despite this, the data clearly highlight the difficulties of measuring adhesion forces for systems of this type. Clearly, to probe viscoelastic effects accurately using the probe microscopy technique

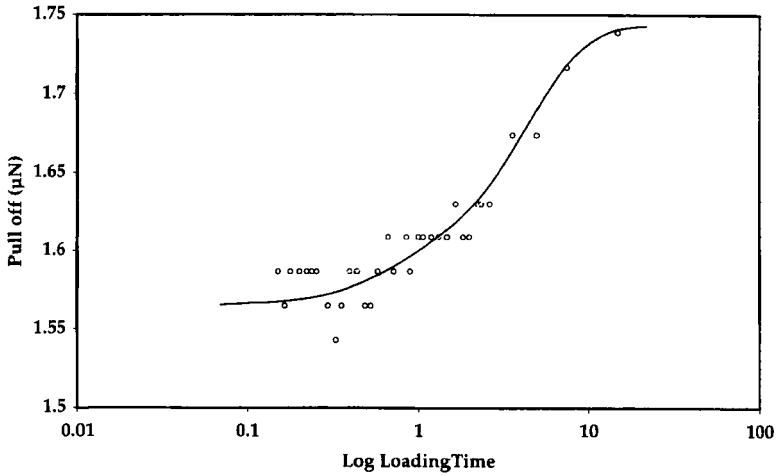

FIGURE 8 The measured pull-off force as a function of loading time at a constant applied load between a 27.2 μm polystyrene sphere and a flat silica substrate.

requires an improved methodology. This is the subject of ongoing research.

Although not planned as such, the fortuitous result of having adhering small particles on the surface of the larger bead has allowed the effects of small surface asperities to be probed in detail. Further experiments are under way in an attempt to control the contact zone better such that controlled amounts of asperity contacts might be introduced.

CONCLUSIONS

Data for the lift-off forces between a single 27 μm polystyrene bead and a flat silica surface have been obtained. Analysis of the contact zone indicated the presence of surface asperities. These asperities are attributed to the presence of small adsorbed polystyrene spheres ($R = 230$ nm). In the contact zone, there are around ten of these spheres. Under the loads applied here, all of these spheres were subjected to significant elasto-plastic deformations. The deformation of these asperities leads to an increasing adhesive pull-off force as a function of load. Control of the contact zone is extremely important in

AFM force measurements. Accurate analysis of the morphology of this zone can allow meaningful comparison of the measured data with established theories. The experimental data collected here also indicate the importance of time-dependent deformations due to viscoelastic creep. Longer contact times resulted in larger contact areas and higher pull-off forces.

Acknowledgment

The authors acknowledge the support of the ARC Special Research Centre for Multiphase Processes.

References

[1] Weeks, B. S., *International J. Molecular Medicine* **1**, 361 (1998).
[2] Mittal, K. L. (Ed.), *Particles on Surfaces 2: Detection, Adhesion, and Removal* (Plenum Press, New York, 1989).
[3] Visser, J., *Particulate Sci. Technol.* **13**, 169 (1995).
[4] Bradley, R. S., *Trans. Far. Soc.* **32**, 1088 (1936).
[5] Derjaguin, B. V., *Kolloid Z.* **69**, 155 (1934).
[6] Krupp, H., *Adv. Colloid Interface Sci.* **1**, 111 (1967).
[7] Johnson, K. L., Kendall, K. and Roberts, A. D., *Proc. R. Soc. London Ser A.* **324**, 301 (1971).
[8] Derjaguin, B. V., Muller, V. M. and Toporov, Yu. P., *J. Colloid Interface Sci.* **53**, 314 (1975).
[9] Tabor, D., *J. Colloid Interface Sci.* **58**, 2 (1977).
[10] Maugis, D., *Colloid Interface Sci.* **150**, 243 (1990).
[11] Johnson, K. L. and Greenwood, J. A., *J. Colloid Interface Sci.* **192**, 326 (1997).
[12] Maugis, D. and Pollock, H. M., *Acta. Metall.* **32**, 1323 (1984).
[13] Hui, C-Y., Baney, J. M. and Kramer, E. J., *Langmuir* **14**, 6570 (1998).
[14] Yoshizawa, H., Chen, Y-L. and Israelachvili, J. N., *J. Phys. Chem.* **97**, 4128 (1993).
[15] Pollock, H. M., *J. Phys. D.* **11**, 39 (1978).
[16] DeMejo, L. P., Rimai, D. S. and Bowen, R. C., *J. Adhesion Sci. Technol.* **2**, 331 (1988).
[17] Rimai, D. S., DeMejo, L. P. and Bowen, R. C., In: *Fundamentals of Adhesion and Interfaces* (VSP, Utrecht, The Netherlands, 1995), pp. 1 - 24.
[18] Thundat, T., Zheng, X-Y., Chen, G. Y., Sharp, S. L., Warmack, R. J. and Schowalter, L. J., *Appl. Phys. Lett.* **63**, 2150 (1993).
[19] Schaefer, D. M., Carpenter, M., Gady, B., Reifenberger, R., DeMejo, L. P. and Rimai, D. S., In: *Fundamentals of Adhesion and Interfaces.* (VSP, Utrecht, The Netherlands, 1995), pp. 35 - 48
[20] Ott, M. L. and Mizes, H. A., *Colloids Surfaces A.* **87**, 245 (1994).
[21] Biggs, S. and Spinks, G., *J. Adhesion Sci. Technol.* **12**, 461 (1998).
[22] Chaudhury, M. K., Weaver, T., Hui, C. Y. and Kramer, E. J., *J. Appl. Phys.* **80**, 30 (1996).
[23] Schaefer, D. M., Carpenter, M., Gady, B., Reifenberger, R., DeMejo, L. P. and Rimai, D. S., *J. Adhesion Sci. Technol.* **9**, 1049 (1995).
[24] Mizes, H. A., *J. Adhesion* **51**, 155 (1995).

[25] Goodwin, J. W., Hearn, J., Ho, C. C. and Ottewill, R. H., *Colloid Polym. Sci.* **252**, 464 (1974)
[26] Method described in detail in Nanoscope III users manual, Appendix 1 (Digital Instruments, Santa Barbara, CA, USA).
[27] Cleveland, J. P., Manne, S., Bocek, D. and Hansma, P. K., *Rev. Sci. Instrum.* **64**, 3583 (1993).
[28] Schultz, J. and Nardin, M., In: *Modern Approaches to Wettability* (Plenum Press, New York, 1992), p. 82.
[29] Overbury, *Chem. Rev.* **75**, 555 (1975).
[30] Rimai, D. S., Moore, R. S., Bowen, R. C., Smith, V. K. and Woodgate, P. E., *J. Mater. Res.* **8**, 662 (1993).
[31] Unertl, W. N., In: *Microstructure and Tribology of Polymers*, Tsukruk, V. V. and Wahl, K. J., Eds. (ACS Books, Washington DC., 1999).